

# UC San Diego

## UC San Diego Previously Published Works

### Title

Mitral Valve Prolapse—The Role of Cardiac Imaging Modalities

### Permalink

<https://escholarship.org/uc/item/1qm1g1mv>

### Journal

Structural Heart, 6(2)

### ISSN

2474-8706

### Authors

Adabifirouzjaei, Fatemeh

Hsiao, Albert

DeMaria, Anthony N

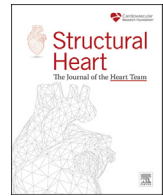
### Publication Date

2022-06-01

### DOI

10.1016/j.shj.2022.100024

Peer reviewed



## Review Article

## Mitral Valve Prolapse—The Role of Cardiac Imaging Modalities

Fatemeh Adabifirouzjaei, MD<sup>a</sup> , Albert Hsiao, MD, PhD<sup>b</sup> ,  
Anthony N. DeMaria, MD<sup>a,\*</sup>

<sup>a</sup> Department of Cardiology, Sulpizio Cardiovascular Center, University of California San Diego, San Diego, California, USA

<sup>b</sup> Department of Radiology, University of California San Diego, San Diego, California, USA

## ARTICLE INFO

## Article history:

Submitted 18 July 2021

Revised 22 October 2021

Accepted 28 October 2021

Guest Editor: Mani Vannan, MBBS, MD

Available online 13 April 2022

## Keywords:

Cardiac computed tomography

Cardiac magnetic resonance images

Echocardiography

Mitral regurgitation

Mitral valve prolapse

Tissue-Doppler imaging

## ABSTRACT

Mitral valve prolapse (MVP) is the most common nonischemic mitral regurgitation etiology and mitral abnormality requiring surgery in the Western world. There is an increasing awareness that pathological findings in MVP are not confined to the valve tissue; rather, it is a complex disease, involving the mitral valve apparatus, cardiac hemodynamics, and cardiac structure. Imaging has played a fundamental role in the understanding of the diagnosis, prevalence, and consequences of MVP. The diagnosis of MVP by imaging is based upon demonstrating valve leaflets ascending into the left atrium through the saddle-shaped annulus. Transthoracic and transesophageal echocardiography are the primary modalities in the diagnosis and assessment of MVP patients and must include careful assessment of the leaflets, annulus, chords, and papillary muscles. High-spatial-resolution imaging modalities such as cardiac magnetic resonance images and cardiac computed tomography play a secondary role in this regard and can demonstrate the anatomical relation between the mitral valve annulus and leaflet excursion for appropriate diagnosis. Ongoing development of new methods of cardiac imaging can help us to accurately understand the mechanism, diagnose the disease, develop an appropriate treatment plan, and estimate the risk for sudden death. Recently, several new observations with respect to prolapse have been derived from cardiac imaging including three-dimensional echocardiography and tissue-Doppler imaging. The aim of this article is to present these new imaging-derived insights for the diagnosis, risk assessment, treatment, and follow-up of patients with MVP.

## ABBREVIATIONS

2D, Two-dimensional; 2D-TTE, Two-dimensional transthoracic echocardiography; 3D, Three-dimensional; 3D-TEE, Three-dimensional transesophageal echocardiography; 3D-TTE, Three-dimensional transthoracic echocardiography; AML, Anterior mitral leaflets; API, Average pixel intensity; BD, Barlow disease; BMVP, Bileaflet MVP; CCT, Cardiac computed tomography; CMRI, Cardiac magnetic resonance images; cVAs, Complex ventricular arrhythmias; EF, Ejection fraction; EROA, Effective regurgitant orifice area; FED, Fibroelastic deficiency; LA, Left atrium; LV, Left ventricle; LVSV, Left ventricular stroke volume; MA, Mitral annulus; MAD, Mitral annular disjunction; MDCTA, Multidetector CT angiography; ML, Mitral leaflet; MR, Mitral regurgitation; MRF, Mitral regurgitant fraction; MVP, Mitral valve prolapse; PISA, Proximal isovelocity surface area; PM, Papillary muscles; PML, Posterior mitral leaflets; SCD, Sudden cardiac death; STE, Speckle-tracking echocardiography; TI, Transillumination; VAs, Ventricular arrhythmias; VCW, Vena contracta width.

## Introduction

Based upon the Carpentier classification,<sup>1</sup> mitral valve prolapse (MVP) is the most common etiology of nonischemic mitral regurgitation (MR). It is a heterogeneous disorder with diversity in pathological, clinical, and imaging presentations.<sup>2</sup> In the Western world, prolapse is

the most common mitral abnormality requiring surgery.<sup>3</sup> Imaging has played a fundamental role in the understanding of the diagnosis, prevalence, and consequences of MVP.

Recently, several new observations with respect to prolapse have been derived from cardiac imaging. The aim of this article is to present these new imaging-derived insights for the

\* Address correspondence to: Anthony N. DeMaria, MD, Division of Cardiovascular Medicine, Sulpizio Cardiovascular Center, University of California San Diego, 9300 Campus Point Drive, MC 7411, La Jolla, CA 92037

E-mail address: [ademaria@ucsd.edu](mailto:ademaria@ucsd.edu) (A.N. DeMaria).

diagnosis, risk assessment, treatment, and follow-up of patients with MVP.

### Mitral Valve Anatomy

The MV apparatus is a complex three-dimensional (3D) structure including anterior (AML) and posterior mitral leaflets (PML), posteromedial and anterolateral papillary muscles (PMs), and chordae tendinae, which attach the inferior surface and free edge of the leaflets to the PMs. The leaflets are suspended from an annulus, which is saddle shaped with 2 superior arcs peaking anteriorly and posteriorly and 2 inferior arcs reaching nadir medially and laterally.<sup>4,5</sup> The annulus is anchored to the left atrium (LA) superiorly and left ventricle (LV) inferiorly. Thus, mitral valve dysfunction may be due to disorders of any of the structures of the apparatus from atrium to ventricle.

The most common classification of mitral leaflet (ML) anatomy is the Carpentier<sup>1</sup> classification. In this classification, the PML is anchored to the fibrous skeleton of the annulus while the AML is contiguous with the aortomitral curtain (intervalvular fibrosa), which is located between the 2 trigones. The PML is typically divided by 2 small clefts into 3 scallops named P1, P2, and P3 and numbered from the anterolateral commissure (near the LA appendage) toward the posteromedial commissure (near the interatrial septum). PML accounts for two-thirds of the mitral annular circumference but only for one-third of the total leaflet area. The AML accounts for one-third of the mitral annular circumference and two-thirds of the total leaflet area. The AML is longer and typically has no visible clefts; to correspond to the scallops of the PML, it is divided into 3 segments: A1, A2, and A3. It is important to note that there is significant variability in the ML anatomy and that variations from the Carpentier system occur in a substantial number of patients.

MVP has been described as being either primary or secondary. Primary MVP is a structural disease of the MLs themselves while secondary MVP results from an imbalance between the size of the leaflets and the volume of the LV.<sup>6</sup> This review will deal only with primary mitral prolapse and the resulting attendant syndrome. The gross pathologic criteria for diagnosing primary MVP are (a) hooding of the intracordal ML structure toward the LA; (b) thickening and elongation of the involved

MLs and subsequent increased valve area; (c) annular dilation present typically with MR<sup>7</sup> (Supplemental Video 1).

### Mitral Annular Disjunction

Mitral annular disjunction (MAD) is a controversial structural abnormality defined as a separation between the annulus and the superior aspect of the LV wall<sup>8</sup> (Figure 1). In this context, the mitral annulus (MA) is not positioned at the junction of the atrium and ventricle but may be displaced above that junction. Accordingly, the disjunctive annulus is decoupled functionally from the ventricle, which may lead to paradoxical annular dynamics with systolic expansion and flattening and significant MR.<sup>9</sup> MAD may account for excessive mobility of the leaflets, visualized as systolic curling, and for the stretch-related myocardial remodeling of the inferobasal wall.<sup>10</sup> LV fibrosis is a very frequent feature of MVP with MAD and can result in an increased incidence of arrhythmias and risk of sudden cardiac death (SCD). Accordingly, MAD has implications for surgical intervention and should be evaluated routinely in MVP patients.<sup>10,11</sup>

The prevalence of actual MAD versus an elongated PML abutting the posterior LA wall remains controversial, as does its relation to MVP. In their original publication, Hutchins and Moore described MAD in a small number of autopsies, with a disproportionate prevalence in MVP subjects and also in otherwise normal subjects.<sup>8</sup> The prevalence of MAD varies in recent studies from 98% to 16% dependent upon the severity of MVP and MR present and the diagnostic modality used.<sup>12,13</sup> It is more prevalent in populations with severe MVP/MR and those studied by transesophageal echo. MAD was detected in both “Barlow disease” (BD) and fibroelastic deficiency (FED) patients, suggesting that it is a primary anatomic abnormality of the annulus. In a recent report, MAD was identified as a risk of progression of the underlying MV disease, although it did not seem to compromise MV surgical reparability.<sup>13</sup> Given the marked variability in the literature, it is clear that the prevalence and clinical significance of MAD need to be studied in a systematic manner in a larger population with a longer follow-up duration.

### Mitral Cleft

Deep clefts are defined as an indentation extending more than half of the depth of the ML. Clefts are to be distinguished from commissures,

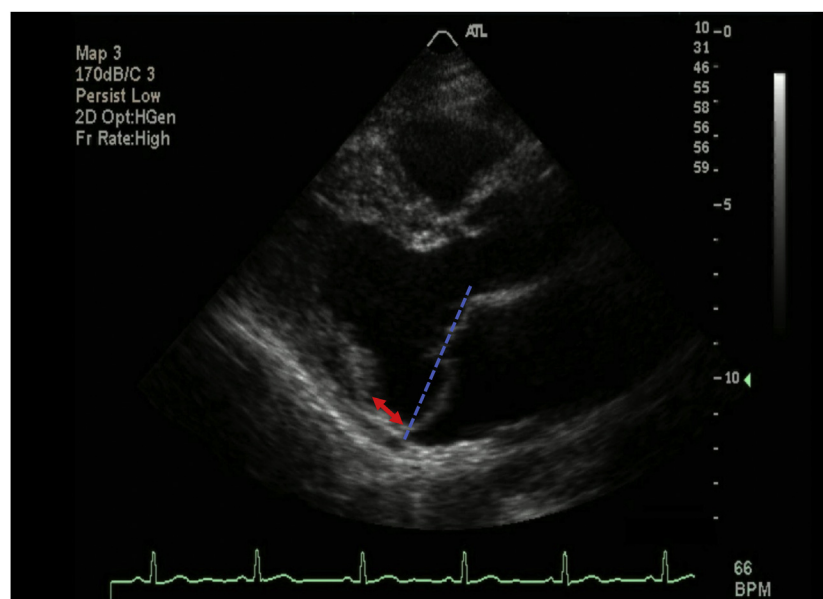


**Figure 1.** Two-dimensional transthoracic echocardiography parasternal long-axis images of a patient with mitral valve prolapse (MVP) + mitral annular disjunction in left ventricle systolic phase. Blue dash lines represent schematic line connecting the posterior and anterior attachment points of mitral leaflets. More than 2 mm displacement of mitral leaflets beyond the annulus identifies MVP. The red arrow represents the length of posterior annular mitral annular disjunction.

which run the entire length of the leaflet, and the normal indentations of the PML dividing it into 3 scallops defined by Ranganathan in 1970.<sup>14</sup> The nomenclature of clefts has varied, as has the prevalence and relation to MVP and, to some extent, the very existence.<sup>15</sup> Ring et al.<sup>16</sup> used 3D transesophageal echocardiography (3D-TEE) to acquire images of normal subjects and MR patients with and without MVP. Clefts were seen in 7 of 57 (12%) normal population, in 64 of 76 (84%) MVP patients, while occurring rarely in patients with alternative causes of MR. Of importance, in 50 patients undergoing surgery (with MVP<sup>38</sup>), they found a close correlation of the findings directly observed at surgery with the 3D echo findings yielding a sensitivity of 93% and a specificity of 92%. In their study, clefts always appear either in prolapsing regions or when framing them and occur in increasing numbers in line with the proportion of the valve that is prolapsing. They concluded that clefts may have an important role in the mechanism of MVP.<sup>16</sup>

**Role of Cardiac Imaging in Understanding the Pathophysiology and Etiology of MVP**

Structural degeneration of the mitral valve has 2 main phenotypes. One phenotype is diffuse myxomatous degeneration, frequently termed BD, which may present as a genetic disorder, while a second markedly different disorder is FED, which appears to be caused by an accelerated aging process.<sup>17,18</sup> While not perfect, clues to distinguish BD from FED have been provided by cardiac imaging, especially echo and cardiac magnetic resonance images (CMRI). BD patients have higher prolapsed volume and height and increased annular dimensions. Also BD patients have bileaflet and multisegmented prolapse with elongated and thick chordae, while FED patients usually have single-leaflet prolapse with focal myxomatous changes in chordae<sup>19,20</sup> (Table 1). While these features may help clinicians differentiate FED from BD, studies are needed to

define the sensitivity and specificity of imaging modalities in discriminating between these two.

Recent studies have identified a “prolapse volume,” consisting of the blood positioned between the MA and the height of the prolapsed leaflets in systole, that is neither part of forward flow nor ejected into the LA at end-systole.<sup>21</sup> For patients with prominent MVP, the Simpson’s method may underestimate the LV end-systolic volume (LVESV) as it only considers the volume located between the apex and the MA and neglects the prolapse volume. This may lead to an underestimation of LVESV, resulting in an overestimation of LV stroke volume (LVSV) and MR.<sup>22</sup> This blood volume is also excluded from the LV systolic volume and the calculated LV ejection fraction (EF).<sup>23</sup> Bach<sup>23</sup> called this phenomenon “the clinical dead pool.” The prolapse volume represents an additional LV volume load beyond that of the regurgitation, which results in an overestimated EF and could lead to discordant LV and LA size.<sup>21,24</sup> Among patients with bileaflet MVP (BMVP), increase of both MR and prolapse volume was associated with proportionate increases in LV diastolic volume.<sup>21</sup>

LV dysfunction is present in a number of MVP patients. Kitkungvan et al.<sup>25</sup> observed that LV fibrosis is more prevalent in CMRI of MVP patients than in other types of MR, suggesting an additional pathophysiology for LV dysfunction beyond that of volume overload. Later, Miller et al.<sup>26</sup> analyzed 20 MVP patients referred for valve repair who underwent hybrid positron emission tomography/magnetic resonance imaging. They found that myocardial segments with fluorodeoxyglucose uptake in MVP patients frequently matched areas of myocardial fibrosis on CMRI. Based on their findings, these authors suggested that an inflammatory component could be prodromal to the development of myocardial fibrosis in MVP,<sup>26</sup> providing a potential target for therapy. An alternate explanation for LV dysfunction in MVP relates to the redundancy and degeneration of the leaflets and the elongation of the chordal apparatus that, together with the dilation and flattening of the MA, result

**Table 1**  
The rules of different echo modalities in characterization of BD and FED

Study	Modality	BD	FED
Chandra et al. <sup>19</sup>	3D-TEE	Billowing height >1 Billowing volume >1.15	Billowing height >1 Billowing volume <1.15
Matsumaru et al. <sup>116</sup>	2D-TTE	Billowing of multiple segments of the leaflets Bileaflet prolapse Elongation or thickening of chorda	Commonly single-leaflet prolapses (most of the time posterior leaflet) - focal myxomatous changes with torn chordae
Clavel et al. <sup>117</sup>	2D-TTE	Bileaflet prolapse Redundant valve tissue with myxomatous degeneration causing prolapse of multiple or all scallops	Posterior prolapse, single-scallop involvement
	3D-TEE	Larger systolic intercommissural and anteroposterior diameters than FED Larger annular dimension than FED Larger mitral leaflet area Larger prolapse volume and height	Dimensions of the mitral annulus remain relatively normal
Apor et al. <sup>118</sup>	3D-TEE	Dilated, remarkably flattened, and hypodynamic annulus	Dilated annulus but relatively preserved saddle-shape and contractile function
Sturla et al. <sup>119</sup>	CMRI	Significantly increased annular dimensions compared to NLs and FED Rounder annular shape cf. to NL and FED Significantly higher prolapse height and volume than FED and NLs Significant difference during systole with an abnormal annular enlargement between mid and late systole	Nonsignificant increased annular dimension compared with NLs. Rounder annular shape compared with NL, lower decrease in eccentricity compared with BD Significantly higher prolapse height and volume than NLs
Kagiyama et al. <sup>120</sup>	3D-TEE	Greater prolapse volume and height than FED Greater prolapse volume to prolapse height ratio (PV/PH) than FED	Lower prolapse volume, height, and PV/PH than BD
Vo et al. <sup>20</sup>	4D-MV Assessment	Significantly increased mitral annular dimensions (area, circumference, interregional distance, septal-lateral distance) compared to FED and secondary MR	Significantly increased mitral annular dimensions (area, circumference, interregional distance, septal-lateral distance) compared with secondary MR

4D-MV, four dimensional mitral valve; BD, Barlow disease; CMRI, cardiac magnetic resonance imaging; FED, fibroelastic deficiency; NL, normal; TEE, transesophageal echocardiography.

in a complex interaction between these structures and the LV. During systole, forces producing mitral closure are transmitted to the chordal apparatus and the PMs, causing abnormal traction and excursion. The MA moves toward the LV apex at peak systole, while the PM tips tend to be drawn in the opposite direction.<sup>25,27,28</sup> Such morphological and mechanical abnormalities might be responsible for a continuous insult to the myocardium and PM stretch, ultimately leading to the development of myocardial hypertrophy and PM or LV fibrosis.<sup>11,29</sup> Focal hypertrophy of the basal LV segments has been demonstrated in MVP and correlated to the excursion of the annulus, suggesting that disproportionately increased regional myocardial function could be responsible for remodeling.<sup>29</sup> Finally, Hei et al.<sup>30</sup> have shown that late systolic MVP on echo is associated with abnormal superior shifts of the MLs and PM during systole. The MV and PM shifts were correlated with an augmented superior force associated with annular dilation and disappeared after surgical MV annuloplasty. These data suggest that MA dilatation may promote secondary superior shifts of the MV contributing to subvalvular PM traction.<sup>30</sup>

### Role of Cardiac Imaging in the Diagnosis, Localization, and Treatment Plan of MVP

Noninvasive imaging modalities are of value in documenting leaflet morphology so as to accurately diagnose MVP and define an appropriate treatment plan.<sup>31,32</sup> Precise definitions of MV morphology and perioperative monitoring of MV anatomy, function, and pathology are essential for successful mitral repair.<sup>33</sup> The historical practice of MV repair based principally on surgical exploration is being transformed into a new standard with shared contributions from both imaging and surgery.<sup>34</sup>

### Echocardiography

For years, 2D-trans thoracic echocardiography (2D-TTE) was the best and standard modality for the diagnosis of MVP.<sup>28,35,36</sup> Multiple 2D-TTE planes provide cross-sectional anatomy of different components of the mitral apparatus.<sup>37</sup> Current echocardiographic criterion for diagnosis includes >2 mm displacement of 1 or both mitral valve leaflets above the annulus within the LA in end-systole.<sup>38</sup> 2D-TTE has very good diagnostic accuracy and high reproducibility in localizing the ML scallops and/or segments.<sup>39</sup> The middle scallop of the PML is the most commonly involved segment in MVP and can easily be observed in the parasternal long-axis view by 2D-TTE (Supplemental Video 1). Lateral scallop prolapse can be seen in the 4-chamber view by 2D-TTE.<sup>40,41</sup> Subsequently, it was found that 2D-TEE was superior to 2D-TTE for diagnosis of MVP and yielded more precise localization<sup>42,43</sup> (Supplemental Video 2). Most

recently, 3D TTE has been found to most accurately identify MVP and quantify the complex 3D-shaped annulus.<sup>44,45</sup>

A comparison of the ability to identify diseased scallops revealed similar sensitivity (94% vs 91%), specificity (100% vs 96%), and accuracy (100% vs 94%) for 3D-TTE and 2D-TEE, respectively.<sup>46</sup> Assessment of the central scallop had the highest accuracy by both 2D-TEE and 3D-TTE methods.<sup>47</sup> However, real-time 3D TEE has now been shown to be superior to any 2D technique and 3D-TTE for identifying the number of prolapsing segments, their location and extent, the presence of flail segments, disparity in scallop heights, regurgitant orifice area, associated ruptured chordae, and commissural dysfunction<sup>44-48</sup> (Figure 2) (Table 2).

Studies employing a multidisciplinary approach to intervention that include imaging protocols for screening, disease severity stratification, and guidance are strongly encouraged at the present time.<sup>34</sup> MV morphology is crucial in determining the feasibility, timing, and complexity of repair<sup>49</sup> (Figure 2). The planning and success of interventional procedures rest on accurate MV anatomic assessment and the detection of those lesions that may predict unsuccessful repair.<sup>50</sup> Quantification of prolapsing or billowing volume, in addition to morphology, can distinguish between more complex versus less important lesions. High-risk criteria would include larger billowing volume, large anterior MV surface area, and multisegmented or bileaflet involvement.<sup>19,34</sup> In this regard, greater agreement has been reported between qualitative assessment of 3D images and surgical findings as compared to 2D images.<sup>51</sup> 3D-TEE has the additional advantage of simulating the surgeon's view and appears to be a significant advance for preoperative and intraoperative use.<sup>52</sup> The 3D zoom image is more commonly utilized in the operating room for evaluation of the MV. In this mode, the acquired image can highlight the precise pathology.<sup>53</sup> Echo-guided MV repair is associated with a higher rate of initial success as well as excellent long-term results relative to the national average for unguided procedures.<sup>34</sup> Repair of posterior leaflet MVP, commonly involving leaflet resection and annuloplasty, has excellent immediate and long-term outcome.<sup>54,55</sup> Central mitral regurgitant jet direction, calcification and marked dilatation of the annulus, and extensive leaflet disease (3 or greater prolapsed or flail segments/scallops seen on intraoperative multiplane TEE) have been shown to be independent predictors of unsuccessful MV repair.<sup>50</sup> The presence of severe bileaflet prolapse or BD was an exclusion criteria for transcatheter edge-to-edge mitral repair in the EVEREST II trial that established the efficacy of this procedure.<sup>56</sup> Although recent studies showed that some devices can be used in the setting of severe bileaflet prolapse, this method requires grasping an extensive amount of hypermobile, redundant leaflet tissue. This may require using multiple clips to address the large regurgitant orifice that is often present, as well as to stabilize clip mobility.<sup>57</sup> This is an evolving

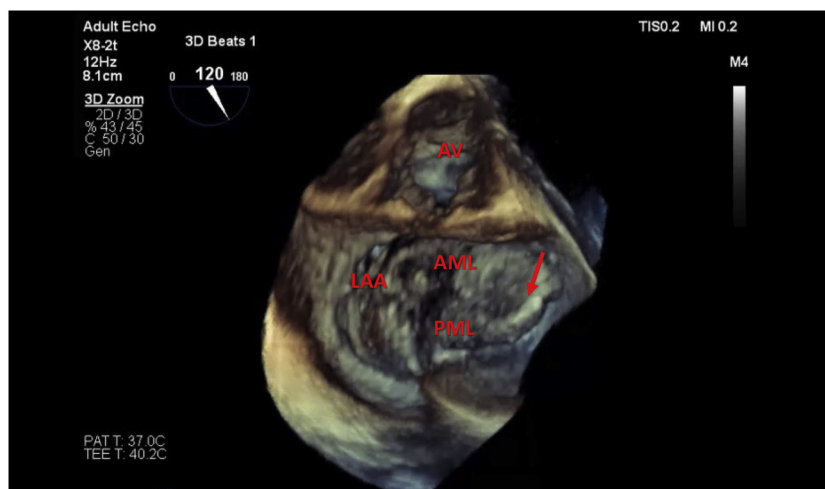


**Figure 2.** Three-dimensional transesophageal echocardiography (3D-TEE) zoom mode acquisition showing en face surgical view of mitral valve with prolapse in the P3 scallop, primarily (red arrow). Leaflet prolapse is diagnosed when there is systolic excursion of the leaflet body into the left atrium due to excess leaflet tissue, with the leaflet-free edge remaining below the plane of the mitral annulus. The mitral valve is oriented with the aortic valve at the 12-o'clock position. Abbreviations: AML, anterior mitral leaflet; AV, aortic valve; LAA, left atrial appendage; PML, posterior mitral leaflet.



**Table 2**  
Studies on various echo modalities and their rules on MVP characterization

Study	Modality	Patients	Findings
García-Orta et al. <sup>44</sup>	2D-TEE-3D-TEE vs surgical findings	MVP-MR undergo surgery	3D accurately classified A1 segment defects, commissural dysfunction. The 2D study incorrectly classified 22 segments, mainly corresponding to complex disease.
Delabays et al. <sup>45</sup>	3D-reconstruction TEE vs surgery	MVP + severe MR	Excellent correspond between echocardiographic localization of prolapse and surgery inspection Excellent correspond between echocardiographic volume of prolapse and surgically resected tissue
Sharma et al. <sup>46</sup>	2D-TEE RT-3D-TEE vs surgical findings	MR undergo surgery	Both modalities were accurate without significant difference
Gutiérrez-Chico et al. <sup>47</sup>	2D-TEE vs 3D-TTE	MVP patients	Segmental analysis is feasible on both modalities with same accuracy
Pepi et al. <sup>51</sup>	2D-TTE, 3D-TTE before surgery 2D-TEE, 3D-TEE during surgery	MVP patients with severe MR	Accuracy in diagnose MV lesion: 3D-TEE (95.6%) > 3D-TTE (90%) and 2D-TEE (87%) > 2D-TTE (77%)
La Canina et al. <sup>121</sup>	2D-TTE, RT-3D-TTE, 2D-TEE, RT-3D-TEE vs. surgical findings	MVP-MR undergo surgery	Accuracy in characterized the MV anatomy and identification of prolapse: RT-3D-TEE (92%) > 2D-TEE (78%) > RT-3D-TTE (52%) > 2D TTE (35%)
Akhter et al. <sup>122</sup>	2D-TEE, 2D-TTE, 3D-MPR Assess the agreement with surgery	MVP who underwent MV repair or replacement	3D-MPR + 2D-TTE: moderately strong agreement for the A2 strong for the A3 AML, P2, PML. 2D-TEE: Moderately strong agreement for A2, AML strong agreement for the P2, PML
Manda et al. <sup>123</sup>	2D-TEE and RT-3D-TEE vs surgical findings	Flail MV + MR/undergo surgery	3D-TEE was superior 2D-TEE in the evaluation of MVP and associated ruptured chordae
Grewal et al. <sup>48</sup>	2D-TEE RT-3D-TEE vs surgical findings	MR undergo MV repair	3D-TEE imaging was superior to 2D-TEE imaging in the diagnosis of P1, A2, A3, and bileaflet disease

Abbreviations: MPR, multiplanar reconstruction; MR, mitral regurgitation; MV, mitral valve; MVP, mitral valve prolapse; TEE, transesophageal echocardiography; TTE, transthoracic echocardiography.

field, and its precise place in the intraoperative imaging algorithm will become established in the next few years.

### Transillumination

Transillumination (TI) is a new 3D tool that improves the visualization of cardiac structures due to shadow effects achieved by the use of a freely movable virtual light to enhance image details and depth.<sup>58</sup> Volpato et al.<sup>59</sup> compared the diagnostic accuracy of TTE-TI side by side with standard 3D-TTE display in 50 patients undergoing surgery for MVP. Surgical valve inspection was used as a reference standard. The correlation of TI with surgery was good for prolapse detection (intraclass correlation [ICC] = 0.78) and chordal rupture localization (ICC = 0.73). The correlation was fair for detection of mitral cleft (ICC = 0.66). Compared with the surgical reference, TI added accuracy to 3D-TTE imaging for the identification of prolapsing scallops (94% vs 89%), chordal rupture (98% vs 92%), and cleft localization (87% vs 54%). They concluded TI modality may contribute to improved personalized pre-surgical planning.<sup>59</sup>

### Cardiac Magnetic Resonance Imaging

Recently, CMRI has emerged as an important noninvasive modality to characterize MVP (Supplemental Video 3). Advantages over echocardiography include the ability for tissue characterization, unlimited imaging planes, no dependency on an acoustic window, and accurate determination of LV volumes and function.<sup>60,61</sup> Also, CMRI may better define MAD of minor degree (MAD < 4 mm)<sup>62</sup> (Figure 3).

However, due to insufficient spatial resolution and volume averaging effect, CMRI failed to demonstrate valve thickening in a recent study.<sup>63</sup> Han et al. analyzed the 2D-TTE and cine CMRI images of 25 MVP patients and 25 healthy volunteers to define diagnostic MVP criteria by CMRI. They demonstrated that CMRI identified MVP by the echo criteria of 2 mm displacement beyond the annulus with 100% sensitivity and

specificity.<sup>115</sup> A reduced signal and darker appearance of the PM have been shown to accurately differentiate MVP from normals and those with conditions involving the mitral subvalvular apparatus.<sup>54</sup> Regarding the role of CMRI in clinical decision-making, it can provide high-resolution volumetric images of the LV, as well as quantitative assessment of regurgitant volume (RV), although compared with 2D-echo, MR fraction and RV measured by CMRI are typically lower.<sup>65,66</sup> CMRI has proven to be accurate in evaluating the annulus dimensions, which may be important whenever an MV prosthesis implantation or repair is planned.<sup>67</sup>

### Cardiac Computed Tomography

Cardiac computed tomography (CCT) provides high-resolution volumetric data sets that can be postprocessed to provide views suitable for MVP diagnosis. After data acquisition, cine reconstruction methods, particularly volume-rendered images, are useful for demonstrating MV structure.<sup>2</sup> The relation between leaflets and annulus can be studied, and the degree of leaflet displacement can be measured. An important advantage of CCT over echocardiography is that it allows for the visualization of adjacent anatomic structures, such as the coronary sinus and coronary arteries, which cannot be easily demonstrated by echocardiogram. Nazari et al.<sup>68</sup> measured the mitral valve leaflet thickness and leaflet billowing of 40 MVP patients who had undergone both TTE and CCT within a 3-month period. In their study, a 68% direct correlation was observed between leaflet thickness measured by TTE and multidetector CT angiography (MDCTA). The correlation between leaflet billowing measured by TTE and MDCTA was 94% ( $p < 0.001$ ). MDCTA measured leaflet billowing with a sensitivity and specificity of 68.4 and 95.2%, respectively, in their study.

Several studies of the diagnostic accuracy of CCT to define the culprit scallop found sensitivities and specificities of 84%-96% and 93%-100%, respectively, compared with echo and had an excellent agreement with operative findings.<sup>69,70</sup> Radiation exposure, poor temporal resolution,

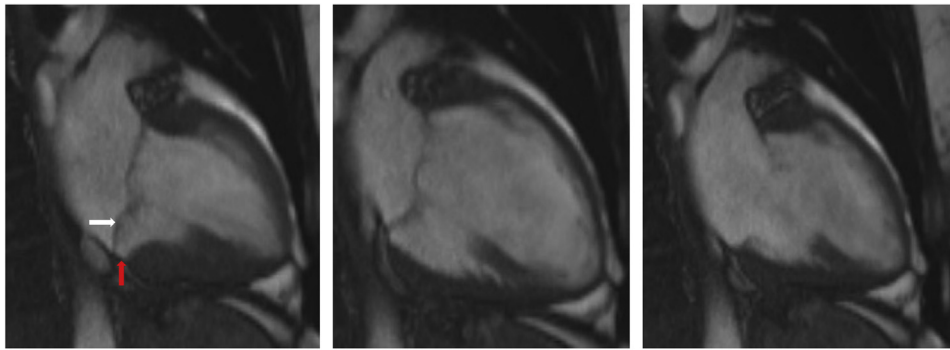


**Figure 3.** Cine cardiac magnetic resonance parasternal images of patients with MVP + MAD during cardiac cycle. The red arrow points to abnormal atrial displacement of mitral valve hinge point which identifies MAD. The white arrow points to more than 2 mm displacement of mitral leaflets beyond the annulus, identifies MVP. Abbreviations: MAD, mitral annular disjunction; MVP, mitral valve prolapse.

and limited ability to examine each leaflet are some of the important limitations of cardiac CCT in the evaluation of MVP<sup>71</sup> although CCT technology has been rapidly evolving in recent years to overcome these historical limitations. While CCT can accurately evaluate LV volume, it is not routinely used to estimate the severity of MR. Thus, although MVP imaging with CCT is possible, it is not used as the primary imaging modality, unless other structural information, such as coronary evaluation, is needed.<sup>69</sup>

### Role of Cardiac Imaging in Risk Stratification of MVP

Prognosis in MVP patients varies widely from a condition with little morbidity and normal life expectancy in half of patients to subsets with high morbidity and mortality directly related to MVP and its complications.<sup>72</sup> The major complications are infective endocarditis, heart failure, stroke, and even SCD.<sup>66,73</sup> Findings that have been observed in MVP-related SCD include left ventricular myocardial fibrosis detected by CMRI or autopsy and complex ventricular ectopy.<sup>74</sup> LV fibrosis, especially near the PM, provides the substrate for the development of ventricular arrhythmias (VAs).<sup>66,75,76</sup> Although the value of routine utilization of CMRI in MVP patients is yet to be studied, in the presence of high-risk factors for arrhythmic MVP such as MAD, marked leaflet redundancy, and repolarization abnormalities, CMRI should probably be performed.<sup>77</sup>

### Echocardiogram

A variety of abnormalities detectable by echo can be prognostic for the occurrence of VAs and SCD. The most common findings in patients who have experienced SCD are bileaflet involvement, high degree of leaflet redundancy, mitral annular dilatation, and leaflet thickness greater than 5 mm. Pathology in other valves, reduced LV function, and larger LA and LV end-systolic diameter also are present in SCD patients.<sup>11,63,73,78,79</sup> MAD by echo, when severe, has been shown to predict the occurrence of nonsustained VAs by significantly disturbing mitral annular function.<sup>80</sup> Although prior studies have shown the correlation between higher MR severity and VAs, a recent systematic review reported that nonsevere MR was present in the majority of patients who experienced cardiac arrest.<sup>81,82</sup> Hourdain et al.,<sup>83</sup> in an international case series, gathered data of 42 resuscitated patients from SCD in whom MVP was the only detectable cause. They observed a common phenotype characterized by syncope, frequent and repetitive premature ventricular contractions originating from the posterior PM, “severe myxomatous MVP disease” defined as combined myxomatous thickened leaflets, BMVP, and MAD. The majority of patients did not have severe MR.<sup>83</sup>

### Speckle-Tracking Echocardiography and Tissue-Doppler Imaging

Speckle-tracking echocardiography (STE) may identify MVP patients at higher risk for VAs by detection of increased mechanical dispersion.<sup>84</sup>

The association between mechanical dispersion and MVP-related arrhythmic complications was reported to be independent of LV systolic function, degree of MR, and type of leaflet involvement. In pediatric patients with MVP,<sup>85</sup> global early diastolic strain by STE was shown to be a sensitive marker of early subtle myocardial injury. Muthukumar et al.<sup>86</sup> examined the pulsed-wave tissue Doppler of 21 myxomatous MVP patients and identified a subset with a spiked high-velocity systolic signal of the lateral annulus of  $\geq 16$  cm/s. This subset did not significantly differ in regard to the severity of prolapse, leaflet thickness, medial annulus Doppler velocity, MR severity, and LVEF. VAs (67% vs 22%) and need of an implantable cardioverter defibrillator (40% vs 0%) were significantly higher in those with the systolic spike. The configuration, which they named the “Pickelhaube” spike, represents altered myocardial deformation and is a risk marker for malignant arrhythmias in patients with myxomatous MVP. They proposed that “the tugging of the posteromedial PM in mid-systole by the myxomatous prolapsing leaflets causes the adjacent posterobasal LV wall to be pulled sharply toward the apex, resulting in the observed spiked configuration.”<sup>86</sup> Subsequently, the highest Pickelhaube signal velocity was found in the posterolateral annulus of BMVP patients, an unconventional site of interrogation.<sup>87</sup> Recently, Muthukumar et al.<sup>86</sup> used STE to identify arrhythmogenic substrate in 44 patients with myxomatous BMVP. They observed that the mean Pickelhaube spike, billowing extent, and basal and mid-lateral wall postsystolic index tend to be higher in patients with malignant arrhythmogenic BMVP. In their study, CMRI evidence of late gadolinium enhancement was reported only in 33% of patients, which suggests that fibrosis occurs at a later stage in the disease. Thus, tissue-Doppler imaging and STE may identify patients at risk of malignant VAs in myxomatous MVP earlier, before the development of fibrosis.<sup>88</sup>

### Cardiac Magnetic Resonance Imaging

CMRI can have a pivotal role in identifying fibrotic myocardial tissue replacement by T1 mapping (T1-map) and abnormal myocardial strain by CMRI feature tracking.<sup>60,89,90</sup> Following gadolinium administration, delayed enhancement and increased extracellular space may represent fibrosis or proteoglycan deposition, both of which are strong predictors of VA events, SCD or heart failure. Therefore, such findings may be useful for clinical decision processes and prognostication.<sup>91,92</sup> Unlike ischemic heart disease or nonischemic cardiomyopathies, even a small focal late gadolinium enhancement burden has been associated with SCD in MVP patients. Basso et al.<sup>66</sup> reviewed the cardiac pathology of 43 patients in whom MVP was the only identifiable cause of SCD. LV fibrosis was detected by histology at the PM level in all patients, and in the inferobasal wall in 88%; suggesting that myocardial stretch by the prolapsing leaflet is the structural hallmark of MVP and may correlate with VAs. Living patients with MVP with and without complex VAs (cVAs) underwent a study protocol including contrast-enhanced CMRI. Patients with either right bundle branch block-type or polymorphic cVAs showed a

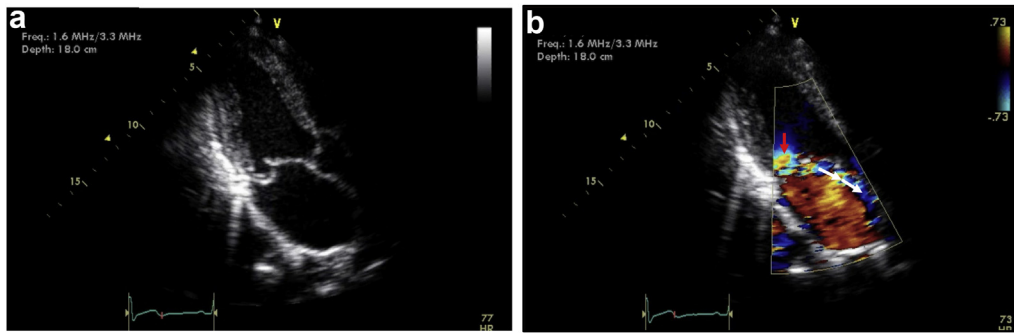


**Figure 4.** Two-dimensional transthoracic echocardiography apical 3-chamber view of a mitral valve prolapse patient with mitral regurgitation. (a) Without and (b) with color Doppler flow. The red arrow points to proximal convergence signal, and white arrows to the eccentricity of the mitral regurgitant jet.

bileaflet involvement in 70% of cases. LV late enhancement was observed to be more intense in MVP patients than in controls (93% vs 14%). Later, Bui et al.<sup>93</sup> showed that MVP may be associated with diffuse late enhancement as suggested by reduced postcontrast T1 times. In their study, diffuse interstitial LV myocardial fibrosis was linked to subclinical systolic dysfunction and may contribute to cVAs in MVP-related MR, even in the absence of focal fibrosis.<sup>93</sup> In the study of Marra et al.,<sup>11</sup> MAD was a constant feature of arrhythmic MVP with LV fibrosis. They identified myocardial hypertrophy and scarring secondary to excessive mobility of the leaflets as a reason of mechanical stretch of the origins of VAs, inferobasal wall and PM.<sup>11</sup>

### Cardiac Imaging and Assessment of MR in MVP

MR in MVP patients may be severe and may result from either progressive myxomatous degeneration or chordal rupture with leaflet flail. MR can cause significant morbidity and mortality.<sup>39,94</sup> CMRI and echocardiography/Doppler imaging are the best modalities for evaluation of MR severity.<sup>95</sup> Published literature has shown general agreement between MR severity assessed on CMRI and on echocardiography/Doppler imaging, but disparity can occur.<sup>72,95,96</sup> Newer technologies, including 4D flow magnetic resonance imaging, are showing promise for improving the reliability of CMRI measurements.<sup>97</sup>

### Echocardiography

TTE is used as a primary tool for the comprehensive assessment of MVP-related MR and can estimate MR severity by using various methods including qualitative (e.g., color Doppler area), semi-quantitative (vena contracta width [VCW]), and quantitative (e.g., proximal isovelocity surface area [PISA] method), the latter to estimate the effective regurgitant orifice area (PISA-EROA) and the RV (PISA-RV)<sup>98</sup> (Figure 4).

There is evidence that these methods can misclassify MR severity, primarily because they measure a single point in time, and since MR is dynamic, the single point in time estimate may not reflect the largest ERO. Enriquez-Sarano et al.<sup>99</sup> observed phasic changes of MR in MVP; from early to mid-late systole, the RV increases due to concomitant increase in both the ERO and the regurgitant velocity. In late systole, despite an increase in regurgitant orifice, the decrease of the ventriculoatrial gradient that was observed results in a decrease in regurgitant velocity. These changes can lead to overestimation of the overall degree of regurgitation, but properly timed measurements made by using the PISA method allow a useful estimation of the overall effective regurgitant orifice.<sup>99</sup> Topilsky et al.<sup>100</sup> observed that assessment of purely mid-late systolic MR in the MVP patient may be misleading because jet area and ERO by flow convergence appear similar to those with holosystolic MR. They thus point out that, for the same ERO, the consequences of the MR (increased RV, LA volume index, and RV

pressure) are less severe/smaller, and the outcomes better in mid-MR to late MR.

Haddad et al.<sup>101</sup> tried to avoid geometric assumptions and take into account the entire systolic cycle and duration of MR by using a novel echocardiographic method that graded MR based on pixel intensity analysis of the continuous-wave Doppler signal. They assessed MR in 290 MVP patients using average pixel intensity (API), color Doppler imaging, VCW, and PISA method. They found that indices of MR severity, such as left ventricular and atrial dimensions and pulmonary arterial pressure, significantly correlate with API severity. The API method showed a linear correlation with color Doppler ( $r = 0.79$ ), VCW ( $r = 0.68$ ), PISA-EROA ( $r = 0.72$ ), and PISA-RV ( $r = 0.67$ ). Additionally, the API showed a stronger intraobserver and interobserver agreement than other methods.<sup>102</sup> However, the API method has not been recognized in published guidelines, and further study is needed to determine the clinical application of this method.

Strain echo by STE is a reliable, angle-independent modality to quantify LV and even LA deformation. Although dependent upon loading, it is independent of myocardial translation and tethering during systolic contraction. As such it is capable of identifying myocardial dysfunction even in the absence of abnormal EF, strain, and has been used in the assessment of MVP patients with MR. Malev et al.<sup>103</sup> compared strain in 58 asymptomatic MVP patients to that of 60 sex- and age-matched healthy subjects. Regional, longitudinal, circumferential, and radial strain, and strain rates were decreased in MVP group only in septal segments. El-Tallawi et al.<sup>104</sup> quantitated patient-specific strain of the MLs in normals and MVP patients, both with and without significant MR, and assessed the determinants of strain by 3D-TEE. Their study showed that prolapsing MV leaflets have higher strain than normal valves, particularly the posterior leaflet. Higher strain measurements were associated with greater MR, as well as larger valves and annuli and increased leaflet thickness. Thus, the underlying MV pathology was the most significant independent determinant of valve deformation in their study.

TEE can also be used in follow-up of MVP-related MR. Ma et al.<sup>105</sup> followed up 82 asymptomatic MVP patients with mild or moderate MR for over a 4.5-year period to evaluate the progression to severe MR. No mild MR progressed to become severe, but 50% of moderate MR progressed to become severe. Only mean MA with a cutoff of 39.6 mm had a good accuracy (area under the curve 0.78, sensitivity 100%, and specificity 63.8%) for progression to severe.<sup>105</sup>

To compare the accuracy of various echocardiographic methods to evaluate MR severity, Yosefy et al.<sup>106</sup> compared 3D-derived vena contracta (VC) area and width, 2D VCW, and effective EROA in 45 patients with more than mild MR. In their study, real time three dimensional echocardiography VC area correlated and agreed well with EROA for both central and eccentric jets. However, real time three dimensional echocardiography overestimated VCW for eccentric jets compared with 3DE and correlated more poorly with EROA, causing clinical



misclassification in 45% of patients with eccentric MR. Overestimation may occur because of the oblique 2D plane relative to the minor axis of the VC, so that the apparent VC width measured is not necessarily the true narrowest neck of the jet<sup>107</sup> (Supplemental Video 4).

### Cardiac Magnetic Resonance Imaging

Assessment of the mechanism of MR, jet direction, and systematic valve mapping is feasible using the CMRI protocol.<sup>108</sup> The preferred CMRI method for MR severity is measuring the mitral RVol computed as the difference between the LVSV and aortic forward SV. However, several alternate methods for quantifying RV with CMRI have been described, including LVSV-PA forward SV; LVSV-RVSV; mitral inflow SV-AO total forward SV.<sup>109-111</sup> Compared with echocardiography, CMRI has several potential advantages for the evaluation of LV volumes, including improved endocardial definition and fewer geometric assumptions.<sup>72</sup> Delleng et al.<sup>112</sup> tried to assess the correlation between MV characteristics and MR severity in MVP patients by using cine CMRI. They assess annular dimensions, maximum systolic anterior and posterior leaflet displacement, PM distance to coaptation point and prolapsed leaflets, as well as diastolic anterior and posterior leaflet thickness and length and LV volumes and mass. They used velocity-encoded CMRI to obtain aortic outflow and to quantify MR volume. In their study, AML length, PML displacement, PML thickness, and the presence of flail are the best CMRI valvular determinants of MVP-related MR.

CMRI helps to quantify MR by using phase-contrast velocity mapping, which, unlike Doppler measurements, are not angle-dependent. CMRI mitral regurgitant fraction (MRF) has the highest diagnostic value to discriminate significant MR.<sup>96,113</sup> The Simpson's method only considers the volume located between the apex and the MA and neglects the prolapsed volume. In severe MVP, this may lead to an underestimation of LVESV and result in an overestimation of LVSV and MR. Vincenti et al.<sup>22</sup> tried to assess the impact of prominent MVP on MR quantification. In patients with MVP (and no more than trace tricuspid regurgitation), MR was quantified by calculating the RV as the difference between LVSV and right ventricular SV. LVSV uncorrected was calculated conventionally as LV end-diastolic volume minus LVESV. A corrected LVESV corrected was calculated as the LVESV plus the prolapsed volume. For MR grading, the 2 methods were concordant in only 34% of patients, as the uncorrected method indicated a 1-grade higher MR severity in 66% patients. In severe BMVP patients, the correction of the LVSV for the prolapse volume is suggested as it modified the assessment of MR severity by 1 grade in a large portion of patients.<sup>22</sup>

Le Goffic et al.<sup>113</sup> tried to evaluate the accuracy of quantitative assessment of MRF by echo and CMRI. MRF by CMRI (volumetric method) and 3D echo MRF have the highest diagnostic value to detect significant MR, whereas the diagnostic value of 2D echo MRF and CMRI-MRF (phase contrast) have been lower.<sup>113</sup> In practice, CMRI should be used as a complementary approach in case of doubt in MR severity after echocardiography or in situations when echocardiography indices are not feasible or suboptimal (i.e., after MV repair or mitral clip procedure, in case of multiple regurgitant jets, periprosthetic leaks, or late-systolic MR.<sup>23,114</sup>

### Conclusion

MVP, the most common etiology of nonischemic MR, is diagnosed by imaging modalities by demonstrating valve leaflets ascending into the LA, passing the saddle-shaped annulus. There is an increasing awareness that pathological findings in MVP are not confined to the valve tissue only and that MVP is a complex disease, which primarily involves the MV apparatus morphology, cardiac hemodynamics, heart chambers dimensions, and ventricular function.

Echocardiography has a central role in diagnosis and assessment of a patient and must include a detailed echocardiogram using high-quality 2D and 3D imaging to define the pathogenesis, involving careful assessment of the leaflets, annulus, chords, and PMs. High-spatial-

resolution imaging modalities such as CMRI and CCT play a secondary role in this regard and can demonstrate the anatomical relation between the MV annular line and leaflet excursion needed for appropriate diagnosis. CMRI is becoming an essential complement to echocardiography for accurate assessment of LV volumes and function, MR quantification, and arrhythmic risk stratification in MVP.

Imaging in MVP is important not only for diagnosis of the disease and assessment of severity of MR but also for prognostic purposes and setting treatment plan. Ongoing development of new methods in cardiac imaging modalities help us to accurately understand the mechanism, diagnose the disease, appropriately plan treatment, and estimating the SCD risk in patients.

### ORCID

Fatemeh Adabifrouzjaei  <https://orcid.org/0000-0001-8521-8911>

Albert Hsiao  <https://orcid.org/0000-0002-9412-1369>

### Funding

The authors received no financial support for this publication.

### Disclosure statement

The authors report no conflicts of interest.

### Supplementary Material

Supplemental data for this article can be accessed on the [publisher's website](#).

### References

- Carpentier A. Cardiac valve surgery: the "French correction." *J Thorac Cardiovasc Surg.* 1983;86(3):323-337. [https://doi.org/10.1016/s0022-5223\(19\)39144-5](https://doi.org/10.1016/s0022-5223(19)39144-5)
- Koo HJ, Yang DH, Oh SY, et al. Demonstration of mitral valve prolapse with CT for planning of mitral valve repair. *Radiographics.* 2014;34(6):1537-1552. <https://doi.org/10.1148/rg.346130146>
- Gammie JS, Chikwe J, Badhwar V, et al. Isolated mitral valve surgery: the Society of Thoracic Surgeons Adult Cardiac Surgery Database analysis. *Ann Thorac Surg.* 2018;106(3):716-727. <https://doi.org/10.1016/j.athoracsur.2018.03.086>
- Witschey WRT, Pouch AM, McGarvey JR, et al. Three-dimensional ultrasound-derived physical mitral valve modeling. *Ann Thorac Surg.* 2014;98(2):961-964. <https://doi.org/10.1016/j.athoracsur.2014.04.094>
- Ryan LP, Jackson BM, Eperjesi TJ, et al. A methodology for assessing human mitral leaflet curvature using real-time 3-dimensional echocardiography. *J Thorac Cardiovasc Surg.* 2008;136(3):726-734. <https://doi.org/10.1016/j.jtcvs.2008.02.073>
- Levine HJ, Isner JM, Salem DN. Primary versus secondary mitral valve prolapse: clinical features and implications. *Clin Cardiol.* 1982;5(6):371-375. <https://doi.org/10.1002/clc.4960050605>
- Guthrie RB, Edwards JE. Pathology of the myxomatous mitral valve. *Nature, secondary changes and complications.* *Minn Med.* 1976;59(9):637-647.
- Hutchins GM, Moore DKS. The association of floppy mitral valve with disjunction of the mitral annulus fibrosus. *N Engl J Med.* 1986;314(9):535-540. <https://doi.org/10.1056/NEJM198602273140902>
- Lee APW, Jin CN, Fan Y, Wong RHL, Underwood MJ, Wan S. Functional implication of mitral annular disjunction in mitral valve prolapse: a quantitative dynamic 3D echocardiographic study. *JACC Cardiovasc Imaging.* 2017;10(12):1424-1433. <https://doi.org/10.1016/j.jcmg.2016.11.022>
- Dejgaard LA, Skjølsvik ET, Lie ØH, et al. The mitral annulus disjunction arrhythmic syndrome. *J Am Coll Cardiol.* 2018;72(14):1600-1609. <https://doi.org/10.1016/j.jacc.2018.07.070>
- Marra MP, Basso C, De Lazzari M, et al. Morphofunctional abnormalities of mitral annulus and arrhythmic mitral valve prolapse. *Circ Cardiovasc Imaging.* 2016;9(8):e005030. <https://doi.org/10.1161/CIRCIMAGING.116.005030>
- Eriksson MJ, Bitkover CY, Omran AS, et al. Mitral annular disjunction in advanced myxomatous mitral valve disease: echocardiographic detection and surgical correction. *J Am Soc Echocardiogr.* 2005;18(10):1014-1022. <https://doi.org/10.1016/j.echo.2005.06.013>
- Mantegazza V, Tamborini G, Muratori M, et al. Mitral annular disjunction in a large cohort of patients with mitral valve prolapse and significant regurgitation. *JACC Cardiovasc Imaging.* 2019;12(11P1):2278-2280. <https://doi.org/10.1016/j.jcmg.2019.06.021>

- 14 Ranganathan N, Lam JH, Wigle ED, Silver MD. Morphology of the human mitral valve. II. The valve leaflets. *Circulation*. 1970;41(3):459-467. <https://doi.org/10.1161/01.CIR.41.3.459>
- 15 Hutchins IM, Schaefer S. Progressive left ventricular noncompaction and systolic dysfunction. *Exp Clin Cardiol*. 2012;17(2):81-83.
- 16 Ring L, Rana BS, Ho SY, Wells FC. The prevalence and impact of deep clefts in the mitral leaflets in mitral valve prolapse. *Eur Heart J Cardiovasc Imaging*. 2013;14(6):595-602. <https://doi.org/10.1093/ehjci/jes310>
- 17 Grau JB, Pirelli L, Yu PJ, Galloway AC, Ostrer H. The genetics of mitral valve prolapse. *Clin Genet*. 2007;72(4):288-295. <https://doi.org/10.1111/j.1399-0004.2007.00865.x>
- 18 Devereux RB, Brown WT, Kramer-Fox R, Sachs I. Inheritance of mitral valve prolapse: effect of age and sex on gene expression. *Ann Intern Med*. 1982;97(6):826-832. <https://doi.org/10.7326/0003-4819-97-6-826>
- 19 Chandra S, Salgo IS, Sugeng L, et al. Characterization of degenerative mitral valve disease using morphologic analysis of real-time three-dimensional echocardiographic images objective insight into complexity and planning of mitral valve repair. *Circ Cardiovasc Imaging*. 2011;4(1):24-32. <https://doi.org/10.1161/CIRCIMAGING.109.924332>
- 20 Vo NM, Van Wijngaarden SE, Ajmone Marsan N, Delgado V, Bax JJ. P5113 assessment of D-shaped annulus of mitral valve in patients with severe mitral regurgitation using semi-automated 4-dimensional analysis: implications for transcatheter interventions. *Eur Heart J*. 2018;39(suppl\_1):1-8. <https://doi.org/10.1093/eurheartj/ehy566.p5113>
- 21 El-Tallawi KC, Kitkungvan D, Xu J, et al. Resolving the disproportionate left ventricular enlargement in mitral valve prolapse due to Barlow disease: insights from cardiovascular magnetic resonance. *JACC Cardiovasc Imaging*. 2020;14(3):573-584. <https://doi.org/10.1016/j.jcmg.2020.08.029>
- 22 Vincenti G, Masci PG, Rutz T, et al. Impact of bileaflet mitral valve prolapse on quantification of mitral regurgitation with cardiac magnetic resonance: a single-center study. *J Cardiovasc Magn Reson*. 2017;19(1):56. <https://doi.org/10.1186/s12968-017-0362-6>
- 23 Bach DS. Dead pool: a non-regurgitant volume overload among patients with Barlow mitral valve prolapse. *JACC Cardiovasc Imaging*. 2020;14(3):585-587. <https://doi.org/10.1016/j.jcmg.2020.09.010>
- 24 Wolff R, Uretsky S. Defining the left ventricular base in mitral valve prolapse: impact on systolic function and regurgitation. *Int J Cardiovasc Imaging*. 2020;36(11):2221-2227. <https://doi.org/10.1007/s10554-020-01927-0>
- 25 Kitkungvan D, Nabi F, Kim RJ, et al. Myocardial fibrosis in patients with primary mitral regurgitation with and without prolapse. *J Am Coll Cardiol*. 2018;72(8):823-834. <https://doi.org/10.1016/j.jacc.2018.06.048>
- 26 Miller MA, Adams DH, Pandis D, et al. Hybrid positron emission tomography/magnetic resonance imaging in arrhythmic mitral valve prolapse. *JAMA Cardiol*. 2020;5(9):1000-1005. <https://doi.org/10.1001/jamacardio.2020.1555>
- 27 Han Y, Peters DC, Kissinger KV, et al. Evaluation of papillary muscle function using cardiovascular magnetic resonance imaging in mitral valve prolapse. *Am J Cardiol*. 2010;106(2):243-248. <https://doi.org/10.1016/j.amjcard.2010.02.035>
- 28 Sanfilippo AJ, Harrigan P, Popovic AD, Weyman AE, Levine RA. Papillary muscle traction in mitral valve prolapse: quantitation by two-dimensional echocardiography. *J Am Coll Cardiol*. 1992;19(3):564-571. [https://doi.org/10.1016/S0735-1097\(10\)80274-8](https://doi.org/10.1016/S0735-1097(10)80274-8)
- 29 Zia MI, Valenti V, Cherston C, Criscito M, Uretsky S, Wolff S. Relation of mitral valve prolapse to basal left ventricular hypertrophy as determined by cardiac magnetic resonance imaging. *Am J Cardiol*. 2012;109(9):1321-1325. <https://doi.org/10.1016/j.amjcard.2011.12.029>
- 30 Hei S, Iwataki M, Onoue T, Nagata Y, Otsuji Y. Possible mechanism of late systolic mitral valve prolapse: systolic superior shift of leaflets secondary to annular dilatation that tracts papillary muscle. *J Am Coll Cardiol*. 2019;316(3):H629-H638. [https://doi.org/10.1016/s0735-1097\(19\)32208-9](https://doi.org/10.1016/s0735-1097(19)32208-9)
- 31 Adams DH, Anyanwu AC. The cardiologist's role in increasing the rate of mitral valve repair in degenerative disease. *Curr Opin Cardiol*. 2008;23(2):105-110. <https://doi.org/10.1097/HCO.0b013e32824fe47>
- 32 Andrawes MN, Feinman JW. 3-Dimensional echocardiography and its role in preoperative mitral valve evaluation. *Cardiol Clin*. 2013;31(2):271-285. <https://doi.org/10.1016/j.ccl.2013.03.005>
- 33 Wei J, Hsiung MC, Tsai SK, et al. The routine use of live three-dimensional transesophageal echocardiography in mitral valve surgery: clinical experience. *Eur J Echocardiogr*. 2010;11(1):14-18. <https://doi.org/10.1093/ejehocard/jep173>
- 34 Drake DH, Zimmerman KG, Hepner AM, Nichols CD. Echo-guided mitral repair. *Circ Cardiovasc Imaging*. 2014;7(1):132-141. <https://doi.org/10.1161/CIRCIMAGING.112.000458>
- 35 Weiss AN, Mims JW, Ludbrook PA, Sobel BE. Echocardiographic detection of mitral valve prolapse. Exclusion of false positive diagnosis and determination of inheritance. *Circulation*. 1975;52(6):1091-1096. <https://doi.org/10.1161/01.CIR.52.6.1091>
- 36 Anthony P, Chandraratna N, Nimalasuriya A, et al. Identification of the increased frequency of cardiovascular abnormalities associated with mitral valve prolapse by two-dimensional echocardiography. *Am J Cardiol*. 1984;54(10):1283-1285. [https://doi.org/10.1016/S0002-9149\(84\)80081-8](https://doi.org/10.1016/S0002-9149(84)80081-8)
- 37 Faletra FF, Leo LA, Paiocchi VL, et al. Anatomy of mitral annulus insights from non-invasive imaging techniques. *Eur Heart J Cardiovasc Imaging*. 2019;20(8):843-857. <https://doi.org/10.1093/ehjci/jez153>
- 38 Levine RA, Triulzi MO, Harrigan P, Weyman AE. The relationship of mitral annular shape to the diagnosis of mitral valve prolapse. *Circulation*. 1987;75(4):756-767. <https://doi.org/10.1161/01.CIR.75.4.756>
- 39 Minardi G, Pino PG, Manzara CC, et al. Preoperative scallop-by-scallop assessment of mitral prolapse using 2D-trans thoracic echocardiography. *Cardiovasc Ultrasound*. 2010;8(1). <https://doi.org/10.1186/1476-7120-8-1>
- 40 Hayek E, Gring CN, Griffin BP. Mitral valve prolapse. *Lancet*. 2005;365(9458):507-518. [https://doi.org/10.1016/S0140-6736\(05\)70275-0](https://doi.org/10.1016/S0140-6736(05)70275-0)
- 41 Dal-Bianco JP, Levine RA. Anatomy of the mitral valve apparatus. Role of 2D and 3D echocardiography. *Cardiol Clin*. 2013;31(2):151-164. <https://doi.org/10.1016/j.ccl.2013.03.001>
- 42 Sochowski RA, Chan KL, Aschaf KJ, Bedard P. Comparison of accuracy of transesophageal versus transthoracic echocardiography for the detection of mitral valve prolapse with ruptured chordae tendineae (flail mitral leaflet). *Am J Cardiol*. 1991;67(15):1251-1255.
- 43 Salustri A, Becker AE, Van Herwerden L, Vletter WB, Ten Cate FJ, Roelandt JRTC. Three-dimensional echocardiography of normal and pathologic mitral valve: a comparison with two-dimensional transesophageal echocardiography. *J Am Coll Cardiol*. 1996;27(6):1502-1510. [https://doi.org/10.1016/0735-1097\(96\)00023-X](https://doi.org/10.1016/0735-1097(96)00023-X)
- 44 García-Orta R, Moreno E, Vidal M, et al. Three-dimensional versus two-dimensional transesophageal echocardiography in mitral valve repair. *J Am Soc Echocardiogr*. 2007;20(1):4-12. <https://doi.org/10.1016/j.echo.2006.07.005>
- 45 Delabays A, Jeanrenaud X, Chassot PG, Von Segesser LK, Kappenberger L. Localization and quantification of mitral valve prolapse using three-dimensional echocardiography. *Eur J Echocardiogr*. 2004;5(6):422-429. <https://doi.org/10.1016/j.euje.2004.03.007>
- 46 Sharma R, Mann J, Drummond L, Livesey SA, Simpson IA. The evaluation of real-time 3-dimensional transthoracic echocardiography for the preoperative functional assessment of patients with mitral valve prolapse: a comparison with 2-dimensional transesophageal echocardiography. *J Am Soc Echocardiogr*. 2007;20(8):934-940. <https://doi.org/10.1016/j.echo.2007.01.028>
- 47 Gutiérrez-Chico JL, Zamorano Gómez JL, Rodrigo-López JL, et al. Accuracy of real-time 3-dimensional echocardiography in the assessment of mitral prolapse. Is transesophageal echocardiography still mandatory? *Am Heart J*. 2008;155(4):694-698. <https://doi.org/10.1016/j.ahj.2007.10.045>
- 48 Grewal J, Mankad S, Freeman WK, et al. Real-time three-dimensional transesophageal echocardiography in the intraoperative assessment of mitral valve disease. *J Am Soc Echocardiogr*. 2009;22(1):34-41. <https://doi.org/10.1016/j.echo.2008.11.008>
- 49 Salgo IS, Gorman JH, Gorman RC, et al. Effect of annular shape on leaflet curvature in reducing mitral leaflet stress. *Circulation*. 2002;106(6):711-717. <https://doi.org/10.1161/01.CIR.0000025426.39426.83>
- 50 Omran AS, Woo A, David TE, Feindel CM, Rakowski H, Siu SC. Intraoperative transesophageal echocardiography accurately predicts mitral valve anatomy and suitability for repair. *J Am Soc Echocardiogr*. 2002. <https://doi.org/10.1067/mje.2002.121534>
- 51 Pepi M, Tamborini G, Maltagliati A, et al. Head-to-Head comparison of two- and three-dimensional transthoracic and transesophageal echocardiography in the localization of mitral valve prolapse. *J Am Coll Cardiol*. 2006;48(12):2524-2530. <https://doi.org/10.1016/j.jacc.2006.02.079>
- 52 Nicoara A, Skubas N, Ad N, et al. Guidelines for the use of transesophageal echocardiography to assist with surgical decision-making in the operating room: a surgery-based approach: from the American Society of Echocardiography in Collaboration with the Society of Cardiovascular Anesthesia. *J Am Soc Echocardiogr*. 2020;33(6):692-734. <https://doi.org/10.1016/j.echo.2020.03.002>
- 53 Lang RM, Addetia K, Narang A, Mor-Avi V. 3-Dimensional echocardiography: latest developments and future directions. *JACC Cardiovasc Imaging*. 2018;11(12):1854-1878. <https://doi.org/10.1016/j.jcmg.2018.06.024>
- 54 Perier P, Stumpf J, Götz C, et al. Valve repair for mitral regurgitation caused by isolated prolapse of the posterior leaflet. *Ann Thorac Surg*. 1997;64(2):445-450. [https://doi.org/10.1016/S0003-4975\(97\)00537-7](https://doi.org/10.1016/S0003-4975(97)00537-7)
- 55 Gillinov AM, Cosgrove DM, Wahi S, et al. Is anterior leaflet repair always necessary in repair of bileaflet mitral valve prolapse? *Ann Thorac Surg*. 1999;68(3):820-824. [https://doi.org/10.1016/S0003-4975\(99\)00805-X](https://doi.org/10.1016/S0003-4975(99)00805-X)
- 56 Mauri L, Garg P, Massaro JM, et al. The EVEREST II trial: design and rationale for a randomized study of the evaluate mitraclip system compared with mitral valve surgery for mitral regurgitation. *Am Heart J*. 2010;160(1):23-29. <https://doi.org/10.1016/j.ahj.2010.04.009>
- 57 Flint N, Price MJ, Little SH, et al. State of the art: transcatheter edge-to-edge repair for complex mitral regurgitation. *J Am Soc Echocardiogr*. 2021;34(10):1025-1037. <https://doi.org/10.1016/j.echo.2021.03.240>
- 58 Genovese D, Addetia K, Kebed K, et al. First clinical experience with 3-dimensional echocardiographic transillumination rendering. *JACC Cardiovasc Imaging*. 2019;12(9):1868-1871. <https://doi.org/10.1016/j.jcmg.2018.12.012>
- 59 Volpato V, Mantegazza V, Tamborini G, et al. Diagnostic accuracy of transillumination in mitral valve prolapse: side-by-side comparison of standard transthoracic three-dimensional echocardiography against surgical findings. *J Am Soc Echocardiogr*. 2020;34(1):98-100. <https://doi.org/10.1016/j.echo.2020.08.017>
- 60 Pradella S, Grazzini G, Miele V. Mitral valve prolapse imaging: the role of tissue characterization. *Quant Imaging Med Surg*. 2020;10(12):2396-2400. <https://doi.org/10.21037/qims-2020-25>
- 61 Parwani P, Avierinos JF, Levine RA, Delling FN. Mitral valve prolapse: multimodality imaging and genetic insights. *Prog Cardiovasc Dis*. 2017;60(3):361-369. <https://doi.org/10.1016/j.pcad.2017.10.007>
- 62 Mantegazza V, Volpato V, Gripari P, et al. Multimodality imaging assessment of mitral annular disjunction in mitral valve prolapse. *Heart*. 2020;107(1):25-32. <https://doi.org/10.1136/heartjnl-2020-317330>
- 63 Suzuki K, Murata M, Yasuda R, et al. Effect of lesional differences in prolapsed leaflets on clinical outcomes in patients with mitral valve prolapse. *Am J Cardiovasc Dis*. 2012;2(3):152-159.

- 64 Scatteia A, Pascale CE, Gallo P, et al. Abnormal papillary muscle signal on cine MRI as a typical feature of mitral valve prolapse. *Sci Rep.* 2020;10(1):9166. <https://doi.org/10.1038/s41598-020-65983-1>
- 65 Lopez-Mattei JC, Ibrahim H, Shaikh KA, et al. Comparative assessment of mitral regurgitation severity by transthoracic echocardiography and cardiac magnetic resonance using an integrative and quantitative approach. *Am J Cardiol.* 2016;117(2):264-270. <https://doi.org/10.1016/j.amjcard.2015.10.045>
- 66 Basso C, Perazzolo Marra M, Rizzo S, et al. Arrhythmic mitral valve prolapse and sudden cardiac death. *Circulation.* 2015;132(7):556-566. <https://doi.org/10.1161/CIRCULATIONAHA.115.016291>
- 67 Naoum C, Blanke P, Cavalcante JL, Leipsic J. Cardiac computed tomography and magnetic resonance imaging in the evaluation of mitral and tricuspid valve disease: implications for transcatheter interventions. *Circ Cardiovasc Imaging.* 2017;10(3):E005331. <https://doi.org/10.1161/CIRCIMAGING.116.005331>
- 68 Nazari M, Khajouei A, Esfahani M, Moradi M. Comparison of the accuracy of cardiac computed tomography angiography and transthoracic echocardiography in the diagnosis of mitral valve prolapse. *Adv Biomed Res.* 2015;4(1):221. <https://doi.org/10.4103/2277-9175.166644>
- 69 Feuchtnr GM, Alkadhhi H, Karlo C, et al. Cardiac CT angiography for the diagnosis of mitral valve prolapse: comparison with echocardiography. *Radiology.* 2010;254(2):374-383. <https://doi.org/10.1148/radiol.2541090393>
- 70 Shah RG, Novaro GM, Blandon RJ, Wilkinson L, Asher CR, Kirsch J. Mitral valve prolapse: evaluation with ECG-gated cardiac CT angiography. *Am J Roentgenol.* 2010;194(3):579-584. <https://doi.org/10.2214/AJR.09.2545>
- 71 Rizvi A, Marcus RP, Guo Y, et al. Dynamic computed tomographic assessment of the mitral annulus in patients with and without mitral prolapse. *J Cardiovasc Comput Tomogr.* 2020;14(6):502-509. <https://doi.org/10.1016/j.jcct.2020.02.005>
- 72 Delling FN, Kang LL, Yeon SB, et al. CMR predictors of mitral regurgitation in mitral valve prolapse. *JACC Cardiovasc Imaging.* 2010;3(10):1037-1045. <https://doi.org/10.1016/j.jcmg.2010.06.016>
- 73 Essayagh B, Sabbag A, Antoine C, et al. Presentation and outcome of arrhythmic mitral valve prolapse. *J Am Coll Cardiol.* 2020;76(6):637-649. <https://doi.org/10.1016/j.jacc.2020.06.029>
- 74 Abraham ZA, Lees DE. Two cardiac arrests after needle punctures in a patient with mitral valve prolapse: psychogenic? *Anesth Analg.* 1989;69(1):126-128. <https://doi.org/10.1213/0000539-198907000-00024>
- 75 Burke AP, Farb A, Tang A, Smialek J, Virmani R. Fibromuscular dysplasia of small coronary arteries and fibrosis in the basilar ventricular septum in mitral valve prolapse. *Am Heart J.* 1997;134(2):282-291. [https://doi.org/10.1016/S0002-8703\(97\)70136-4](https://doi.org/10.1016/S0002-8703(97)70136-4)
- 76 Yang LT, Ahn SW, Li Z, et al. Mitral valve prolapse patients with less than moderate mitral regurgitation exhibit early cardiac chamber remodeling. *J Am Soc Echocardiogr.* 2020;33(7):815-825.e2. <https://doi.org/10.1016/j.echo.2020.01.016>
- 77 Pelliccia A, Sharma S, Gati S, et al. 2020 ESC Guidelines on sports cardiology and exercise in patients with cardiovascular disease. *Eur Heart J.* 2021;42(1):17-96. <https://doi.org/10.1093/eurheartj/ehaa605>
- 78 Sriram CS, Syed FF, Ferguson ME, et al. Malignant bileaflet mitral valve prolapse syndrome in patients with otherwise idiopathic out-of-hospital cardiac arrest. *J Am Coll Cardiol.* 2013;62(3):222-230. <https://doi.org/10.1016/j.jacc.2013.02.060>
- 79 Düren DR, Becker AE, Dunning AJ. Long-term follow-up of idiopathic mitral valve prolapse in 300 patients: a prospective study. *J Am Coll Cardiol.* 1988;11(1):42-47. [https://doi.org/10.1016/0735-1097\(88\)90164-7](https://doi.org/10.1016/0735-1097(88)90164-7)
- 80 Carmo P, Andrade MJ, Aguiar C, Rodrigues R, Gouveia R, Silva JA. Mitral annular disjunction in myxomatous mitral valve disease: a relevant abnormality recognizable by transthoracic echocardiography. *Cardiovasc Ultrasound.* 2010;8:53. <https://doi.org/10.1186/1476-7120-8-53>
- 81 Kligfield P, Hochreiter C, Kramer H, et al. Complex arrhythmias in mitral regurgitation with and without mitral valve prolapse: contrast to arrhythmias in mitral valve prolapse without mitral regurgitation. *Am J Cardiol.* 1985;44(13):1545-1549. [https://doi.org/10.1016/0002-9149\(85\)90970-1](https://doi.org/10.1016/0002-9149(85)90970-1)
- 82 Narayanan K, Uy-Evanado A, Teodorescu C, et al. Mitral valve prolapse and sudden cardiac arrest in the community. *Heart Rhythm.* 2016;13(2):498-503. <https://doi.org/10.1016/j.hrthm.2015.09.026>
- 83 Hourdain J, Clavel MA, Deharo JC, et al. Common phenotype in patients with mitral valve prolapse who experienced sudden cardiac death. *Circulation.* 2018;138:1067-1069. <https://doi.org/10.1161/CIRCULATIONAHA.118.033488>
- 84 Ermakov S, Gulhar R, Lim L, et al. Left ventricular mechanical dispersion predicts arrhythmic risk in mitral valve prolapse. *Heart.* 2019;105(14):1063-1069. <https://doi.org/10.1136/heartjnl-2018-314269>
- 85 Çelik SF. Early impairment left ventricular mechanics in children with mitral valve prolapse. *Am J Cardiol.* 2019;123(12):1992-1998. <https://doi.org/10.1016/j.amjcard.2019.03.009>
- 86 Muthukumar L, Rahman F, Jan MF, et al. The Pickelhaube sign: novel echocardiographic risk marker for malignant mitral valve prolapse syndrome. *JACC Cardiovasc Imaging.* 2017;10(9):1078-1080. <https://doi.org/10.1016/j.jcmg.2016.09.016>
- 87 Ignatowski D, Schweitzer M, Pesek K, et al. Pickelhaube spike, a high-risk marker for bileaflet myxomatous mitral valve prolapse: Sonographer's quest for the highest spike. *J Am Soc Echocardiogr.* 2020;33(5):639-640. <https://doi.org/10.1016/j.echo.2020.02.004>
- 88 Muthukumar L, Jahangir A, Jan MF, et al. Left ventricular global and regional deformation in arrhythmic myxomatous bileaflet mitral valve prolapse syndrome. *JACC Cardiovasc Imaging.* 2020;13(8):1842-1844. <https://doi.org/10.1016/j.jcmg.2020.02.035>
- 89 Guglielmo M, Fusini L, Muscogiuri G, et al. T1 mapping and cardiac magnetic resonance feature tracking in mitral valve prolapse. *Eur Radiol.* 2020;31(2):1100-1109. <https://doi.org/10.1007/s00330-020-07140-w>
- 90 Edwards NC, Moody WE, Yuan M, et al. Quantification of left ventricular interstitial fibrosis in asymptomatic chronic primary degenerative mitral regurgitation. *Circ Cardiovasc Imaging.* 2014;7(6):946-953. <https://doi.org/10.1161/CIRCIMAGING.114.002397>
- 91 Levine RA, Durst R. Mitral valve prolapse. A deeper look. *JACC Cardiovasc Imaging.* 2008;1(3):304-306. <https://doi.org/10.1016/j.jcmg.2008.04.003>
- 92 Pradella S, Grazzini G, Brandani M, et al. Cardiac magnetic resonance in patients with mitral valve prolapse: focus on late gadolinium enhancement and T1 mapping. *Eur Radiol.* 2019;29(3):1546-1554. <https://doi.org/10.1007/s00330-018-5634-5>
- 93 Bui AH, Roujol S, Foppa M, et al. Diffuse myocardial fibrosis in patients with mitral valve prolapse and ventricular arrhythmia. *Heart.* 2017;103(3):204-209. <https://doi.org/10.1136/heartjnl-2016-309303>
- 94 Singh RG, Cappucci R, Kramer-Fox R, et al. Severe mitral regurgitation due to mitral valve prolapse: risk factors for development, progression, and need for mitral valve surgery. *Am J Cardiol.* 2000;85(2):193-198. [https://doi.org/10.1016/S0002-9149\(99\)00645-1](https://doi.org/10.1016/S0002-9149(99)00645-1)
- 95 Uretsky S, Gillam L, Lang R, et al. Discordance between echocardiography and MRI in the assessment of mitral regurgitation severity: a prospective multicenter trial. *J Am Coll Cardiol.* 2015;65(11):1078-1088. <https://doi.org/10.1016/j.jacc.2014.12.047>
- 96 Suri RM, Vanoverschelde JL, Grigioni F, et al. Association between early surgical intervention vs watchful waiting and outcomes for mitral regurgitation due to flail mitral valve leaflets. *JAMA.* 2013;310(6):609-616. <https://doi.org/10.1001/jama.2013.8643>
- 97 Hsiao A, Lustig M, Alley MT, Murphy MJ, Vasanaawala SS. Evaluation of valvular insufficiency and shunts with parallel-imaging compressed-sensing 4D phase-contrast MR imaging with stereoscopic 3D velocity-fusion volume-rendered visualization. *Radiology.* 2012;265(1):87-95. <https://doi.org/10.1148/radiol.12120055>
- 98 Ommen SR, Mital S, Burke MA, et al. 2020 AHA/ACC guideline for the diagnosis and treatment of patients with hypertrophic cardiomyopathy: a report of the American College of Cardiology/American Heart Association Joint Committee on clinical practice guidelines. *Circulation.* 2020;142:e558-e631. <https://doi.org/10.1161/CIR.0000000000000937>
- 99 Enriquez-Sarano M, Sinak LJ, Tajik AJ, Bailey KR, Seward JB. Changes in effective regurgitant orifice throughout systole in patients with mitral valve prolapse. *Circulation.* 1995;92(10):2951-2958. <https://doi.org/10.1161/01.cir.92.10.2951>
- 100 Topilsky Y, Michelena H, Bichara V, Maalouf J, Mahoney DW, Enriquez-Sarano M. Mitral valve prolapse with mid-late systolic mitral regurgitation: pitfalls of evaluation and clinical outcome compared with holosystolic regurgitation. *Circulation.* 2012;125(13):1643-1651. <https://doi.org/10.1161/CIRCULATIONAHA.111.055111>
- 101 El Haddad M, De Backer T, De Buyzere M, et al. Grading of mitral regurgitation based on intensity analysis of the continuous wave Doppler signal. *Heart.* 2017;103(3):190-197. <https://doi.org/10.1136/heartjnl-2016-309510>
- 102 Kamoen V, El Haddad M, De Backer T, De Buyzere M, Timmermans F. The average pixel intensity method and outcome of mitral regurgitation in mitral valve prolapse. *J Am Soc Echocardiogr.* 2020;33(1):54-63. <https://doi.org/10.1016/j.jecho.2019.07.021>
- 103 Malev E, Zemtsovsky E, Pshepiy A, Timofeev E, Reeve S, Prokudina M. Evaluation of left ventricular systolic function in young adults with mitral valve prolapse. *Exp Clin Cardiol.* 2012;17(4):165-168. <https://doi.org/10.6084/m9.figshare.1104384.v1>
- 104 El-Tallawi KC, Zhang P, Azencott R, et al. Valve strain quantitation in normal mitral valves and mitral prolapse with variable degrees of regurgitation. *JACC Cardiovasc Imaging.* 2021;14(6):1099-1109. <https://doi.org/10.1016/j.jcmg.2021.01.006>
- 105 Ma JI, Igata S, Strachan M, et al. Predictive factors for progression of mitral regurgitation in asymptomatic patients with mitral valve prolapse. *Am J Cardiol.* 2019;123(8):1309-1313. <https://doi.org/10.1016/j.amjcard.2019.01.026>
- 106 Yosely C, Hung J, Chua S, et al. Direct measurement of vena contracta area by real-time 3-dimensional echocardiography for assessing severity of mitral regurgitation. *Am J Cardiol.* 2009;104(7):978-983. <https://doi.org/10.1016/j.amjcard.2009.05.043>
- 107 Hall SA, Brickner ME, Willett DL, Irani WN, Afridi I, Grayburn PA. Assessment of mitral regurgitation severity by Doppler color flow mapping of the vena contracta. *Circulation.* 1997;95(3):636-642. <https://doi.org/10.1161/01.cir.95.3.636>
- 108 Gabriel RS, Kerr AJ, Raffel OC, Stewart RA, Cowan BR, Occlshaw CJ. Mapping of mitral regurgitant defects by cardiovascular magnetic resonance in moderate or severe mitral regurgitation secondary to mitral valve prolapse. *J Cardiovasc Magn Reson.* 2008;10(1):16. <https://doi.org/10.1186/1532-429X-10-16>
- 109 Zoghbi WA, Adams D, Bonow RO, et al. Recommendations for noninvasive evaluation of native valvular regurgitation: a report from the American Society of Echocardiography developed in collaboration with the Society for Cardiovascular Magnetic Resonance. *J Am Soc Echocardiogr.* 2017;30(4):303-371. <https://doi.org/10.1016/j.jecho.2017.01.007>
- 110 Hsiao A, Tariq U, Alley MT, Lustig M, Vasanaawala SS. Inlet and outlet valve flow and regurgitant volume may be directly and reliably quantified with accelerated, volumetric phase-contrast MRI. *J Magn Reson Imaging.* 2015;41(2):376-385. <https://doi.org/10.1002/jmri.24578>
- 111 Feneis JF, Kyubwa E, Atianzar K, et al. 4D flow MRI quantification of mitral and tricuspid regurgitation: reproducibility and consistency relative to conventional MRI. 2018;48(4):1147-1158. <https://doi.org/10.1002/jmri.26040>
- 112 Delling FN, Rong J, Larson MG, et al. Evolution of mitral valve prolapse: insights from the Framingham Heart Study. *Circulation.* 2016;133(17):1688-1695. <https://doi.org/10.1161/CIRCULATIONAHA.115.020621>



- 113 Le Goffic C, Toledano M, Ennezat PV, et al. Quantitative evaluation of mitral regurgitation secondary to mitral valve prolapse by magnetic resonance imaging and echocardiography. *Am J Cardiol.* 2015;116(9):1045-1410. <https://doi.org/10.1016/j.amjcard.2015.07.064>
- 114 Zoghbi WA, Asch FM, Bruce C, et al. Guidelines for the evaluation of valvular regurgitation after percutaneous valve repair or replacement: a report from the American Society of Echocardiography developed in collaboration with the Society for Cardiovascular Angiography and Interventions, Japanese Society of Echocardiography, and Society for Cardiovascular Magnetic Resonance. *J Am Soc Echocardiogr.* 2019;32(4):431-475. <https://doi.org/10.1016/j.echo.2019.01.003>
- 115 Han Y, Peters DC, Salton CJ, et al. Cardiovascular magnetic resonance characterization of mitral valve prolapse. *JACC, Cardiovasc Imag.* 2008;1(3):294-303. <https://doi.org/10.1016/j.jcmg.2008.01.013>
- 116 Matsumaru I, Eishi K, Hashizume K, et al. Clinical and pathological features of degenerative mitral valve disease: billowing mitral leaflet versus fibroelastic deficiency. *Ann Thorac Cardiovasc Surg.* 2014;20(6):987-994. <https://doi.org/10.5761/atcs.0a.13-00168>
- 117 Clavel M-A, Mantovani F, Malouf J, et al. Dynamic phenotypes of degenerative myxomatous mitral valve disease: quantitative 3-dimensional echocardiographic study. *Circ Cardiovasc Imaging.* 2015;8(5):e002989. <https://doi.org/10.1161/circimaging.114.002989>
- 118 Apor A, Nagy A, Kovacs A, et al. Three-dimensional dynamic morphology of the mitral valve in different forms of mitral valve prolapse - potential implications for annuloplasty ring selection. *Cardiovasc Ultrasound.* 2016;14(1):32. <https://doi.org/10.1186/s12947-016-0073-4>
- 119 Sturla F, Onorati F, Puppini G, et al. Dynamic and quantitative evaluation of degenerative mitral valve disease: A dedicated framework based on cardiac magnetic resonance imaging. *J Thorac Dis.* 2017:S225-S238. <https://doi.org/10.21037/jtd.2017.03.84>
- 120 Kagiya N, Toki M, Hayashida A, et al. Prolapse volume to prolapse height ratio for differentiating barlow's disease from fibroelastic deficiency. *Circ J.* 2017;1730-1735. <https://doi.org/10.1253/circj.cj-16-1291>
- 121 La Canna G, Arendar I, Maisano F, et al. Real-time three-dimensional transesophageal echocardiography for assessment of mitral valve functional anatomy in patients with prolapse-related regurgitation. *Am J Cardiol.* 2011;107(9):1365-1374. <https://doi.org/10.1016/j.amjcard.2010.12.048>
- 122 Akhter N, Zhao Q, Andrei A-C, et al. Identification of prolapsing mitral valve scallops by a three-dimensional multiplanar reconstruction method. *Echocardiography.* 2015; 32(1):106-113. <https://doi.org/10.1111/echo.12608>
- 123 Manda J, Kesanolla SK, Hsuing MC, et al. Comparison of real time two-dimensional with live/real time three-dimensional transesophageal echocardiography in the evaluation of mitral valve prolapse and chordae rupture. *Echocardiography.* 2008; 25(10):1131-1137. <https://doi.org/10.1111/j.1540-8175.2008.00832.x>